DNA−Poly(diallyldimethylammonium chloride) Complexation and Transfection Efficiency

Manuel Alatorre-Meda,*,† Pablo Taboada,‡ Barbara Krajewska,§ Markus Willemeit,|| Alexander Deml,|| Roland Klösel,|| and Julio R. Rodríguez*,†

Grupo de Nanomateriales y Materia Blanda, Departamento de Física de la Materia Condensada, Facultad de Física, Universidad de Santiago de Compostela, E-15782 Santiago de Compostela, Spain; Grupo de Física de Coloides y Polímeros, Departamento de Física de la Materia Condensada, Facultad de Física, Universidad de Santiago de Compostela, E-15782 Santiago de Compostela, Spain; Faculty of Chemistry, Jagiellonian University, 30-060 Kraków, Ingardena 3, Poland; and Biontex Laboratories GmbH, D-82152 Martinsried/Planegg, Germany

Received: February 24, 2010; Revised Manuscript Received: June 9, 2010

The present work assesses the influence of the cationic charge density (CD) and the cationic valence of poly(diallyldimethylammonium chloride) (pDADMAC) on the DNA compaction and subsequent transfection. Four homopolymers (CD = 1, with different valences) and one copolymer, poly(acrylamide-*co*-diallyldimethylammonium chloride) (coDADMAC) (CD < 1, equivalent in valence to one of the homopolymers), were studied. The characterization of the DNA−pDADMAC complexes (polyplexes) as a function of the polycation nitrogen to DNA phosphate molar ratios, *N*/*P*, was done by means of conductometry, electrophoretic mobility (ζ-potential), dynamic light scattering (DLS), isothermal titration calorimetry (ITC), atomic force microscopy (AFM), and β-galactosidase (ONPG) and luciferase expression assays at 25 °C and physiological pH. In general, all polyplexes rendered compact and stable structures ($R_H \sim 100$ nm) with positive surface charges (∼11 mV) but low transfection efficiencies. As revealed by ITC, the DNA−pDADMAC complexation was characterized by a high binding affinity, the process being entropically driven. In particular, two characteristic ratios ((*N*/*P*)c and (*N*/*P*)*) were detected. Conductometry and ITC data demonstrated that the DNA compaction ratio, (*N*/*P*)c, was mainly governed by CD. Meanwhile the ratio from which the polyplex size remained constant, (*N*/*P*)*, was found to be valence-dependent as revealed by DLS. On the other hand, the low transfer rate of the polyplexes appeared to be correlated with the high binding affinity observed throughout the complexation process and with a core−shell structure the complexes presumably adopt.

I. Introduction

The interactions of DNA with cationic compounds in mixed solutions lead to the formation of interesting chemical constructs that are of special importance for gene therapy.[1] Therein, the compounds serve as vectors for DNA transfection. DNA transfection consists of the successful transfer and expression of extracellular genetic material to the nucleus of eukaryotic cells and is done with the aim of replacing defective or adding missing genes.[2] Transfection requires the use of vectors that guarantee (i) DNA compaction, (ii) DNA protection against enzymatic attacks in the vicinity of the cell membrane, and (iii) DNA delivery across the membrane with efficiency and specificity. The most efficient transfection vectors known to date are based on viruses; however, they suffer from severe limitations such as host immune responses.[3] Due to their stability on storage and ease of production, in conjunction with targetability and with the potential of being administered repeatedly with minimal host immune response, nonviral delivery systems for gene therapy have been proposed for years now as safer alternatives to viral vectors.[2,4−6] Two major types of nonviral vectors currently investigated are cationic lipids and cationic polymers, of which DNA−polycation complexes, also referred to as polyplexes, have proven to be more stable even in very dilute solutions.[7,8]

Polyelectrolytes are polymers with ionizable groups that, in polar solvents, such as water or acidic solutions, dissociate leaving ions on the polymer chain and counterions in the solution.[9,10] Upon mixing, oppositely charged polyelectrolytes interact electrostatically and form complexes in a process that is promoted by an increase in entropy which is due to a release of counterions.[11,12] Accordingly, polycation characteristics such as valence, charge density, and structure may be expected to have an important impact on the DNA compaction and subsequent transfection. Cationic polymers most commonly studied as gene carriers include chitosan, polyethylenimine (PEI), poly(L-lysine) (pLL), poly(β-amino ester)s, and poly(amidoamine) dendrimers (refs 13−15 and references therein). In addition, because of its permanent cationic charge, poly(diallyldimethylammonium chloride) (pDADMAC) has recently been explored.[16,17]

pDADMAC is a water-soluble cationic polymer that has been widely used in technical applications as a flocculant agent and as a composite for biosensors.[18−20] pDADMAC is obtained by a cyclopolymerization as schematized in Figure 1. At low conversions, the polymerization results in strictly linear polymer chains composed of configurational isomers of pyrrolidinium rings; whereas at higher conversions (i.e., commercial samples) branching of pendent allylic double bonds can proceed.[18−22]

* Authors to whom correspondence should be addressed. E-mail: manuel_alatorre@yahoo.com.mx (M.A.-M.); jr.rodriguez@usc.es (J.R.R.).
† Grupo de Nanomateriales y Materia Blanda, Universidad de Santiago de Compostela.
‡ Grupo de Física de Coloides y Polímeros, Universidad de Santiago de Compostela.
§ Jagiellonian University.
|| Biontex Laboratories GmbH.

10.1021/jp1016856
Published on Web 07/07/2010

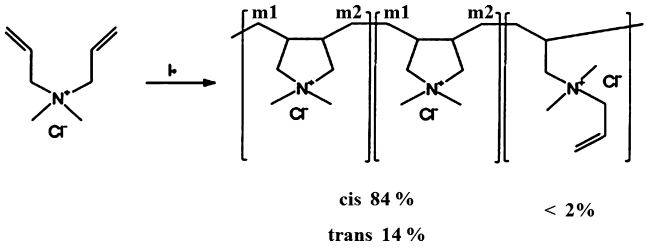

Figure 1. Scheme of the polymerization of diallyldimethylammonium chloride stopped at low conversions.

The physical structure of pDADMAC is special provided that the polymer chain possesses two methylene groups connecting the repeat units. The methylene groups are separated in turn by a short distance (either m1 to m1 or m2 to m2 in Figure 1). Both the branching and the physical structure provide pDADMAC with a high flexibility compared to other polycations.[23,24]

The present work assesses the influence of the charge density and the valence of pDADMAC on the DNA compaction and transfection at physiological pH and 25 °C by means of conductometry, electrophoretic mobility (ζ-potential), dynamic light scattering, isothermal titration calorimetry, atomic force microscopy, and β-galactosidase (ONPG), and luciferase expression assays. The characterization of the DNA−pDADMAC complexes as a function of the pDADMAC nitrogen to DNA phosphate molar ratios, *N*/*P*, was done in terms of the conductance, ζ-potential, hydrodynamic radius R_H, time-dependent stability, thermodynamics of binding, morphology, and transfection efficiency. Four homopolymers (CD = 1, with different valences) and one copolymer, poly(acrylamide-*co*-diallyldimethylammonium chloride) (coDADMAC) (CD < 1, equivalent in valence to one of the homopolymers), were studied.

II. Experimental Section

A. Materials. ***Cationic Polymers.*** Poly(diallyldimethylammonium chloride) homopolymers of very low molecular weight (<100 kDa), of low molecular weight (100−200 kDa), of medium molecular weight (200−350 kDa), of high molecular weight (400−500 kDa), and poly(acrylamide-*co*-diallyldimethylammonium chloride) copolymer (250 kDa) were purchased from Sigma-Aldrich.

DNA and Plasmids. Calf thymus DNA sodium salt with a reported molecular weight of 10−15 million Da was from Sigma-Aldrich. Plasmids pCMV-Lac-Z (7 kbp, 1 mg mL^{-1}, suspended in water for injection, WFI), and pCMV-Luc (6 kbp, 1 mg mL^{-1}, suspended in WFI) were from PlasmidFactory. The purity of DNA and plasmids was tested by UV−vis spectroscopy in which the ratio of the absorbance of a DNA stock solution at 260 nm to that at 280 nm was found to be 1.9, demonstrating that DNA was free of proteins.[25]

Physicochemical Characterization. Bis-Tris and EDTA (both with a purity grade of 99%) from Sigma Aldrich were used as a buffer and as a quelant, respectively.

Transfection Experiments. Metafectene Pro transfection reagent (MEP) and HeLa cells were from Biontex Laboratories GmbH, IZB/Planegg/Germany. NaCl, KCl, and KH_2PO_4 from Roth, and $Na_2HPO_4 \cdot 2H_2O$ from Applichem were used to prepare the phosphate buffered saline buffer (PBS). Dulbecco's modified Eagle's Media (DMEM) and Fetal Calf Serum (FCS) both from PAA were used as culture medium and culture medium additive, respectively.

ONPG Assay for β-Galactosidase Expression. KH_2PO_4, K_2HPO_4, KCl, $MgSO_4$, and 2-β-mercaptoethanol (used to prepare the buffer A), Na_2CO_3 (used to prepare the stop solution), and ONPG substrate were from Applichem. TRIS and Igepal CA-630 (used to prepare the ONPG buffer) were from Roth and from Sigma-Aldrich, respectively.

Luciferase Expression Assay. Na_3PO_4, EDTA, and 1% Triton X-100, (used to prepare the lysis buffer) were from Applichem. ATP sodium salt$\cdot 3H_2O$, $MgCl_2$, and DDT (all from Applichem) and tricine (from SERVA) were used to prepare the ATP solution. Tricine, $MgCl_2$, DDT, and D-luciferin (from P.J.K.) were employed to prepare the luciferin solution.

Protein Concentration. BCA reagents (Reagent A and Reagent B) were from Thermo Scientific.

All materials were used as received. Water purified in a 18 MΩ cm Milli-Q Plus water system was used throughout the work.

B. Sample Preparation. The repeat unit molecular weights considered for the calculations of valence, molar concentration (either in nitrogen units for pDADMACs and coDADMAC or in nucleotide units for DNA), and *N*/*P* were 161.5, 374.5, and 330 g mol^{-1} for pDADMAC, coDADMAC, and DNA,[26] respectively. (It has to be noted that the molecular weight of the coDADMAC repeat unit results from the sum of three molecules of monomer acrylamide (AM) plus one molecule of the monomer DADMAC considering the copolymer composition of 45 wt % DADMAC reported by Sigma-Aldrich).

The sample preparation was as follows.

Physicochemical Characterizations. Unless otherwise stated, polymers and DNA were dissolved in separate in a 10 mM Bis Tris-EDTA buffer, pH of 6.5. A series of polyplexes with compositions of $0.02 \leq N/P \leq 10$, were prepared by adding the polymer solutions of desired concentrations to a 0.061 mM DNA solution, both solutions being equal in volume. For conductometry experiments, the Bis-Tris−EDTA buffer and DNA concentrations were 2 and 0.303 mM, respectively. For the ITC experiments, the DNA concentration in the cell amounted to 0.303 mM, whereas the concentration of the polymer solutions in the injector amounted to 17.4 mM.

Transfection Assays. Plasmids, polymers, and MEP were dissolved separately in 10 mM PBS (1×PBS), pH 7.4. A series of polyplexes with compositions of $1 \leq N/P \leq 18$ were prepared. The DNA−MEP lipoplex, used as a positive blank, was prepared in a ratio MEP to DNA of 4:1 (μL:μg). DNA concentration amounted to 0.091 mM (0.03 μg μL^{-1}).

Once mixed, the samples were incubated for at least 20 min at room temperature to reach the complexation prior to transfection.

C. Conductometry. Conductance data were collected with a SevenMulti conductivity meter from Mettler Toledo. The dip-type conductance cell used was calibrated by measuring the conductivity of a series of standard solutions of KCl at different concentrations. The cell constant was determined to be equal to 0.139 cm^{-1}. To perform the study, 20 mL of a reservoir solution (containing either DNA or pure buffer) were placed in a conductivity cell that was continuously stirred; then, aliquots of pDADMAC solutions were added. The cell calibration and measurements were made at 25.00 ± 0.01 °C in a Julabo thermostat bath. The instrument measured the changes in the conductance of the solution and, once the standard deviation of the measurements was lower than 0.4%, it displayed the conductance value. DNA dilution after each polymer injection was considered for the *N*/*P* calculations.

D. Electrophoretic Mobility Measurements. Electrophoretic mobility was obtained with a Zetasizer NanoSeries (Malvern) using folded capillary cells. The instrument measures the

electrophoretic mobility of the particles and converts it to the ζ-potential using the classical Smoluchowski expression:[27]

$$\alpha = \frac{\varepsilon\zeta}{\eta} \tag{1}$$

where α, ε, ζ, and η denote the electrophoretic mobility, permittivity of the media, ζ-potential of the particles, and viscosity of the media, respectively. All measurements were carried out at 25 °C. The results are the average of five measurements.

E. Dynamic Light Scattering Measurements. DLS measurements were performed in a Spectrometer Autosizer 4800 from Malvern Instruments equipped with a Uniphase 75 mW Ar laser operating at 488 nm with vertically polarized light. Each time correlation was processed by a digital autocorrelator PCS7132 from Malvern Instruments. The data analyses were performed by means of the ALV-NonLin Data Analysis Software Package, on the basis of the well-known CONTIN method.[28] A detailed description of the data analysis is given elsewhere.[29] Briefly, the diffusion coefficient, D, was determined from the intensity correlation function, $g_2(\tau)$; then, the hydrodynamic radius was calculated according the well-known Stokes−Einstein equation:[30]

$$D = \frac{k_B T}{6\pi\eta R_H} \tag{2}$$

where k_B is the Boltzmann constant, T the absolute temperature, η the solvent viscosity, and R_H the particle hydrodynamic radius. All measurements were carried out at 25.00 ± 0.01 °C, and at a scattering angle of 90°. In order to study the stability of the complexes with time, the samples were stored at 4 °C during the testing time (7 days); before each test, they were left for 15 min at 25 °C inside the instrument to achieve thermal stabilization. The results are the average of five runs of 60 s.

F. Isothermal Titration Calorimetry (ITC). Binding studies were performed using a VP-ITC titration microcalorimeter from MicroCal Inc., Northampton, MA, with a cell volume of 1.355 mL at 25 °C. Samples were degassed in a ThermoVac system (MicroCal) prior to use. The sample cell was filled with the DNA solution and the reference cell with buffer solution only. Polymer solutions were introduced into the thermostated cell by means of a syringe and stirred at 250 rpm, which ensured rapid mixing but did not cause foaming on solutions. Each titration consisted of an initial 2 μL injection (neglected in the analysis) followed by 55 subsequent 5 μL injections programmed to occur at 400 s intervals, sufficient for the heat signal to return to the baseline. We present the results of the ITC experiments in terms of the enthalpy change per injection, ΔH_i, as a function of the N/P molar ratios. Heats of dilution from titrations of polymer solutions into buffer only (without DNA) were subtracted from the heats obtained from titrations of the polymer solutions into the DNA solution to obtain the net binding heats. All experiments were carried out in duplicate and the reproducibility was within ±3%.

Raw ITC data of polymers binding to DNA were processed as described previously.[31] The isotherms were fitted by using the two-binding-site model supplied by MicroCal (Origin v. 5.0). This model employs the following fitting equation that incorporates Langmuir isotherm binding equilibria for two independent types of association, where Q is the heat per injection, M is the macromolecule concentration, V is the volume of the cell, n and ΔH are the stoichiometry and enthalpy of complexation, respectively, Θ is the fraction of ligand bound to the macromolecule, and the subindices next to each parameter stand for the corresponding sets of sites 1 and 2:

$$Q = MV(n_1\Theta_1\Delta H_1 + n_2\Theta_2\Delta H_2) \tag{3}$$

One can solve for Θ using the equilibria equations for binding constants K_1 and K_2, X being the concentration of ligand and $[X]$ the concentration of free ligand:

$$K_1 = \frac{\Theta_1}{(1-\Theta_1)[X]} \quad \text{and} \quad K_2 = \frac{\Theta_2}{(1-\Theta_2)[X]} \qquad [X] = X - M(n_1\Theta_1 + n_2\Theta_2) \tag{4}$$

To achieve an accurate fit of all six floating parameters to our data, multiple attempts were performed starting from different initial parameters. The same six values were reached at the minimum χ^2, regardless of the values of initialization.

G. Atomic Force Microscopy Measurements. Tapping Mode AFM in air was performed with a Multimode SPM (Nanoscope IIIa, Digital Instruments). For imaging, the polyplexes were diluted 10-fold in the Bis-Tris−EDTA buffer as compared to the DLS experiments. The samples were deposited on freshly cleaved mica, left for incubation during 2 min and dried by capillarity immediately after. The experiments were run using a J tube scanner (scan size 10 × 10 μm; vertical range 5 μm). Microfabricated crystal silicon probes with a spring constant of 20−80 N/m and a resonant frequency of 281−319 kHz (Veeco MPP-11100) were used as received. Z-scale accuracy was checked once a day by means of a silicon grating (TGZ02 silicon grating, from Ultrasharp Cantilevers and Gratings) ensuring a nominal height deviation lower than 2% at the highest scan size. To eliminate imaging artifacts, the scan direction was varied to ensure a true image. The images were obtained from at least five macroscopically separated areas on each sample. All images were processed using procedures for plane-fit and flatten in the WSxM 4.0 Develop 11.4 software[32] without any filtering. All experiments were carried out at room temperature.

H. Transfection Efficiency. Transfection experiments were performed in triplicate. HeLa cells with an optical confluence of 80−90% were seeded into wells (1.0 cm^2) of a 48-well plate (200 μL, 1 × 10^5 cells/well) and grown at standard culture conditions (DMEM supplemented with 10% FCS in an atmosphere of 10% CO_2 at 37 °C) for 24 h. Afterward, the complexes formed as described before were added and incubated for 6 h at standard culture conditions. Then, the medium containing the complexes was exchanged with fresh medium and cells were incubated for further 42 h. Finally, (i) the β-galactosidase and (ii) the luciferase expressions as well as (iii) the total protein concentration per well were determined as follows.

(i) ONPG Assay for β-Galactosidase Expression. The culture medium was discarded, and the cells were washed with 1×PBS. The cells were then shaken at room temperature (240 rpm, 15 min) in the presence of 120 μL of lysis buffer (0.25 M TRIS (pH 7.8), 0.6% Igepal CA 630). Once the cells were lysed, 120 μL of 1×PBS were added and homogenized by pipetting up and down several times. Meanwhile, an aliquot of 20 μL was separated for the protein content determination, the remaining 220 μL of cell lysate were mixed with 250 μL of buffer A (100 mM KH_2PO_4/K_2HPO_4 (pH 7.5), 10 mM KCl, 1 mM $MgSO_4$,

TABLE 1: pDADMACs Employed for DNA Complexation[a]

	average M_w (kDa)	label
homopolymers	<100	p(1,<619)
	150	p(1,929)
	275	p(1,1703)
	450	p(1,2786)
copolymer	250	p(0.26,668)

[a] In $p(x,y)$, x and y stand for charge density and valence, respectively.

and 50 mM 2-β-mercaptoethanol). Then, 60 μL of ONPG substrate solution (10 mg mL^{-1} ONPG in 100 mM $Na_2HPO_4 \cdot 2H_2O$, pH 7.5) were added to the mixture and incubated at room temperature until the solution became yellow (8 min). After incubation, the reaction was terminated by the addition of 500 μL of stop solution (1 M Na_2CO_3). Then, in order to get rid of any precipitate that could appear, the samples were cooled down at 4 °C for 15 min and warmed up at room temperature for several minutes. Finally, the absorbance of the samples was measured at 405 nm with an ELx800 Absorbance Microplate Reader from Biotek. The analysis was carried out at room temperature in nonsterile conditions.

(ii) Luciferase Expression Assay. The culture medium was discarded, and the cells were washed with 1×PBS. In this case, the cells were handled above a refrigerated gel pack to maintain the temperature around 4 °C. The cells were shaken (240 rpm, 30 min) in the presence of 100 μL of lysis buffer (100 mM Na_3PO_4 (pH 7.8), 2 mM EDTA (pH 8), 1% Triton X-100). In order to avoid debris after lysation, the cell lysates were homogenized by taking off and refilling a constant volume of 80 μL several times. Then, as in the β-galactosidase assay, 20 μL of cell lysate were separated for the protein content determination. The remaining 80 μL were mixed with 80 μL of ATP solution (30 mM tricine, 3 mM ATP, 0.225 mM $MgCl_2$, 1 mM DDT) and shaken (320 rpm, 5 min). Finally, 40 μL of each well were transferred to an opaque white plate and measured for 1 s for their luminescence in the presence of luciferin solution (0.5 mM D-luciferin, 30 mM tricine, 0.225 mM $MgCl_2$, 1 mM DDT). The analysis was carried out under nonsterile conditions. The luminescence determination was performed with a MicroLumat Plus Luminometer from Berthold Technologies.

(iii) Protein Concentration. The protein concentrations of the cell lysates were determined via the BCA assay. The 20 μL aliquots separated from the previous assays were mixed with 400 μL of BCA solution (98% reagent A). Both samples from β-galactosidase and luciferin assays were incubated first at the standard culture conditions (the former for 30 min and the latter for 90 min), and second at room temperature (both samples for 15 min). After incubation, the absorbance of the samples was measured at 562 nm. The absorbance determination was carried out at nonsterile conditions with the same instrument as for the β-galactosidase assay.

III. Results and Discussion

The CD of a polycation is defined as the mole fraction of the ionized groups along the polymer chain. Consequently, while for pDADMACs the CD equals 1 in all cases, for coDADMAC it amounts to 0.26 based on the composition reported by Sigma-Aldrich. The valence by contrast, defined as the total charge per polymer chain, was calculated as the ratio of the average polymer molecular weight, M_w, divided by the molecular weight of its repeat unit. Table 1 summarizes the cationic polymers employed in the present study with the nomenclature cited throughout this work.

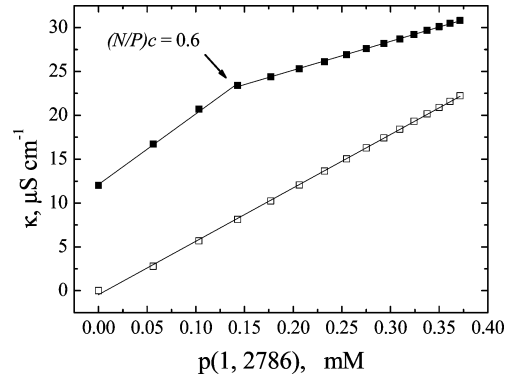

Figure 2. Specific electrical conductance, κ, of p(1,2786) as a function of the polycation concentration. Filled and empty squares stand for polycation addition to a DNA and to a pure buffer solution, respectively.

The complex formation is a process dominated by electrostatics; in consequence, a careful electrochemical study of the polyplexes in solution is strongly recommended to better understand the interactions. The next two sections will detail the electrochemical analysis that was done at two levels: (i) the bulk, by means of conductometric experiments (section 3.1), and (ii) the surface charge of the polyplexes formed, by means of electrophoretic mobility experiments (section 3.2).

3.1. Conductometry. Upon mixing, oppositely charged compounds interact electrostatically and form complexes in a process that is promoted by an increase in entropy due to a release of counterions.[11,12] The tracking of this release by means of conductometry has been used to assess the zone at which DNA and cationic vectors such as surfactants,[33] and liposomes[34] interact. In the present paper, we measured the change in conductance originated from the addition of pDADMAC and coDADMAC solutions to both DNA and pure buffer solutions.

A representative plot of the specific electrical conductance κ as a function of the polycation concentration, recorded for p(1,2786), is presented in Figure 2. The filled and empty squares stand for the DNA and pure buffer (reservoir) solutions, respectively. κ was calculated from the experimental specific conductance, κ_{exp}, and corrected for the specific conductance of the buffer solution, κ_0, according to $\kappa = \kappa_{exp} - \kappa_0$. As observed, in the buffer solution alone the conductivity increased linearly with the concentration of p(1,2786) (empty squares), indicating that no aggregation took place under the whole range of the polycation concentration. In the DNA solution (filled squares) by contrast, the conductivity grew linearly, however, with a clear change in slope at the polycation concentration of 0.142 mM, corresponding to the *N*/*P* ratio of 0.6. It can be concluded that, at the polycation concentrations below the inflection point, electrostatic interactions between the positive charges of p(1,2786) and the negative charges of DNA give rise to a coupled release of counterions, Na^+ from DNA and Cl^- from p(1,2786), thereby justifying the increase in conductivity. Once the change occurred, a lower slope is observed since only the counterions coming from the polycation dissociation now contributed to the conductivity of the solution.[34] For this reason, the inflection point is then considered as the point from which DNA is compacted. A similar behavior was found for the other polymers tested. The results are summarized in Table 2.

From Table 2 it is apparent that the ratio at which DNA completely compacted, (*N*/*P*)c, is governed by the charge density rather than by the valence. Also, the (*N*/*P*)c of pDADMACs

TABLE 2: Characteristic *N*/*P* Ratios and Hydrodynamic Radii, R_H, of Polyplexes[a]

polymer	(*N*/*P*)c	(*N*/*P*)*	R_H (nm)
p(1,<619)	0.7	4	79.4 ± 2.1
p(1,929)	0.6	2	87.0 ± 6.9
p(1,1703)	0.7	2	108.9 ± 12.5
p(1,2786)	0.6	1	112.6 ± 9.7
p(0.26,668)	1.5	2	199.8 ± 23.5

[a] (*N*/*P*)c and (*N*/*P*)* stand for the DNA compaction ratio (determined by conductometry) and for the ratio from which the size of the polyplexes remain constant (determined by DLS), respectively. R_H are calculated in the range (*N*/*P*)* ≤ *N*/*P* ≤ 10.

polyplexes are lower than half the (*N*/*P*)c of the coDADMAC polyplex. A similar result was achieved by our group for DNA−chitosan polyplexes in which the lower was the pH of the medium the lower became the concentration of chitosan needed for complexation.[29]

3.2. Electrophoretic Mobility. When DNA interacts with cationic vectors, the negative charge is expected to diminish or even to shift to positive, a phenomenon that facilitates its approach and uptake trough the cell membrane during transfection.[35−38] For many polyplexes, the crossover from a negative to a positive ζ-potential (known as isoelectric point) occurs at or very close to the isoneutrality point (*N*/*P*)φ.[39] (*N*/*P*)φ is defined as the point at which the *N*/*P* molar ratio of the polyplex equals 1, that is, the ratio where the negative charges of DNA are stoichiometrically neutralized by the positive charges of the polycation.[13] In the present study, the characterization was done in the range 0.2 ≤ *N*/*P* ≤ 10 for all polyplexes. Table 3 summarizes the ζ-potential values obtained for the polyplexes as a function of their *N*/*P* molar ratios.

The data in this table reveal that all pDADMAC polyplexes show positive ζ-potential values at *N*/*P* ≥ 1, thereby providing evidence for a complete DNA compaction along this region. It can also be observed that regardless of their different valences, all pDADMAC polyplexes reach a plateau around 12 mV which is in good agreement with other systems including poly(amino acid)s[40] and cationic polymers in either linear configurations or dendrimer structures.[39] By contrast, the negative to positive shift in the charge of DNA for the coDADMAC polyplex begins from *N*/*P* = 2. In compliance with other systems encompassing grafted hydrophilic chains,[13] this result suggests that the presence of the neutrally charged acrylamide in the backbone of the cationic polymer chain makes necessary the use of a higher quantity of vector to reach the isoelectric point. However, the maximum value of ζ-potential remains around 12 mV as those of the pDADMAC polyplexes, demonstrating that AM linked to DADMAC (at least at the molar fraction chosen for this study) does not decrease the polyplex positive charge recommended for transfection as it occurred with other grafted copolymers.[41−43]

On the other hand, the decreasing trend in the modulus of the negative ζ-potentials at 0.2 ≤ *N*/*P* ≤ 1 for all polyplexes (*N*/*P* < 2 for the coDADMAC complex) reveals the gradual neutralization of the negatively charged phosphate groups of DNA as the concentration of the cationic vector increased. Very importantly, in respect of the zone where DNA is expected to be compacted, the ζ-potential results demonstrate that the isoelectric point is close to the (*N*/*P*)c suggested by conductometry.

Likewise, it is apparent that at the ratios where the ζ-potentials remain almost constant, those well above (*N*/*P*)φ, the polyplexes adopt the core−shell structure described in section 3.6.

3.3. Dynamic Light Scattering. In addition to the overall charge, the proper uptake of polyplexes by the cell through endocytosis is governed by their size intended to be equivalent to that of a virus. In this context, the characterization of the DNA−pDADMAC polyplexes in terms of the size was carried out by means of DLS. The study was done in two steps. First, the hydrodynamic radii of the polyplexes, R_H, were determined at 0.2 ≤ *N*/*P* ≤ 10. And second, the evolution of R_H with time was followed for the polyplexes at *N*/*P* = 10.

Figure 3 depicts the change in R_H of polyplexes as a function of the *N*/*P* molar ratio in the region 1 ≤ *N*/*P* ≤ 10. It has to be noted that the values of R_H for *N*/*P* < 1 are not reported for any of the polyplexes because the intensity correlation functions (from which R_H is calculated) were weak, baseline-absent, and nonreproducible. Similar results have previously been supported by the fact that linear particles are hardly detected by DLS.[29,30] Moreover, the baseline absence of the correlation functions has also been ascribed to the presence of two or more populations related to a gradual coil−globule transition during DNA compaction.[44]

The plots in Figure 3 show that except p(1,2786) all the polyplexes exhibit a common behavior in that their size at the isoneutrality point, *N*/*P* = 1, is bigger than at the other *N*/*P* ratios. In this regard, by using different types of cationic polymers, it has been shown that, at low values of *N*/*P* (<1), water-soluble polyplexes with a net negative charge exist. Upon increasing the concentration of the cationic polymer, strongly polydisperse aggregates of polyplexes are formed as a result of the lowered negative charge, with the largest aggregates existing at a value of *N*/*P* close to 1. Finally, a further increase in the polycation concentration reduces the size of the polyplexes due to electrostatic repulsion (ref 13 and references therein). In consequence, for the polycation-mediated DNA compaction there must be one ratio from which polyplexes are more suitable for gene therapy; that is, a ratio from which they have the most compact structural configuration with possible polyplex−polyplex interactions being avoided. Indeed, as can be seen from Figure 3, all polyplexes under examination showed one characteristic ratio (*N*/*P*)* from which their sizes were practically constant. The value of (*N*/*P*)* follows a decreasing trend with pDADMAC valence of the polyplexes, with p(1,619) and p(1,2786) showing the highest and the lowest (*N*/*P*)* values of 4 and 1, respectively, the other polyplexes showing the (*N*/*P*)* value of 2. The (*N*/*P*)* values and the average sizes of the polyplexes calculated from the data plotted in Figure 3 in the range (*N*/*P*)* ≤ *N*/*P* ≤ 10 are listed in Table 2.

The data in Figure 3 also reveal that there are two distinct size regions, one for the pDADMAC polyplexes, CD = 1, whose sizes are in the range 80 < R_H < 120 nm, and another one for the coDADMAC polyplex, CD = 0.26, whose size is ca. 200 nm, once the DNA compaction is achieved. Within the group of pDADMAC polyplexes, the average polyplex size increases with the increasing cationic valence of pDADMAC. Although it may be expected that due to its higher valence, a pDADMAC with a higher molecular weight can interact with DNA better and condense it more efficiently than a pDADMAC of a lower valence, it appears that the electrostatic interactions are outweighed to a certain extent by a decrease in the polycation solubility. This was previously demonstrated for DNA−chitosan polyplexes.[29,45] We reported that chitosan-mediated DNA polyplexes followed a linear trend with chitosan valence (molecular weight), and accordingly the sizes of 187 ± 21, 210 ± 11, and 246 ± 13 nm were obtained for low-, middle-, and high-molecular-weight chitosan, respectively.[29] Concerning the coDADMAC polyplex, its size is larger than that of pDADMAC polyplexes in the whole concentration range. This behavior can

TABLE 3: ζ-Potential of Polyplexes (in mV) Measured at Different *N/P* Molar Ratios

N/P	p(1,<619)	p(1,929)	p(1,1703)	p(1,2786)	p(0.26,668)
0.2	−45.0 ± 3.2	−44.3 ± 1.9	−43.1 ± 0.7	−39.9 ± 3.0	−41.4 ± 2.3
0.4	−44.6 ± 1.4	−33.3 ± 1.4	−35.4 ± 2.2	−41.2 ± 3.5	−35.5 ± 1.3
0.6	−35.3 ± 1.4	−34.3 ± 3.5	−33.6 ± 2.0	−40.6 ± 1.3	−34.0 ± 6.0
0.8	−29.0 ± 5.5	−24.0 ± 5.4	−16.4 ± 12.0	−22.3 ± 2.6	−24.0 ± 1.6
1	7.7 ± 0.8	10.5 ± 0.8	10.1 ± 0.5	11.8 ± 1.1	−19.9 ± 1.9
2	11.8 ± 0.7	12.2 ± 0.1	11.2 ± 0.4	11.8 ± 0.6	12.7 ± 0.3
4	11.7 ± 1.3	10.5 ± 0.8	13.1 ± 0.6	12.0 ± 0.7	11.5 ± 0.2
6	12.2 ± 0.5	12.0 ± 0.5	12.0 ± 0.3	11.9 ± 0.3	10.6 ± 0.5
10	11.8 ± 0.3	12.0 ± 0.3	11.9 ± 0.4	12.8 ± 0.1	12.3 ± 0.1

be a consequence of a lower amount of negatively charged phosphate groups in DNA neutralized by the positive counterparts of coDADMAC, and thus DNA is expected not to be completely compacted. Similar results have been also reported for other polymers. For instance, copolymers made of cationic and hydrophilic monomers inhibited the DNA condensation as demonstrated by Toncheva et al.[41] The authors show that, compared to pLL homopolymer, in the formation of pLL-*gr*-pEG, pLL-*gr*-dextran, and pLL-*gr*-pHPMA polyplexes, pLL was slightly hampered in its ability to condense DNA and consequently higher concentrations of the grafted copolymers were required to quench the fluorescence of ethidium bromide attached to DNA. In our system, we think the presence of AM in the polycation chain is also responsible for the bigger sizes of the coDADMAC polyplex. It is because of the well-known high hydrophilic capacity of AM[46,47] that may allow larger amounts of water to be housed in the polyplex interior.

From the R_H data, and their analysis and interpretation presented in this section, it can be concluded then that, unlike (*N*/*P*)c, the R_H and (*N*/*P*)* values are mainly influenced by the cationic valence of pDADMAC. In this context, it is of additional interest the fact that the values of (*N*/*P*)c and (*N*/*P*)* are in reasonably good agreement with those obtained for this system by means of agarose gel electrophoresis.[16] To highlight the interplay between (*N*/*P*)c and (*N*/*P*)*, the authors provided evidence of DNA with different complexation states along the transition from the former to the latter ratio.

On the other hand, taking into account that polyplex stability is a key issue in gene therapy, in this study we followed the stability of the polyplexes with time for one of the formulations above (*N*/*P*)c for each polymer. Figure 4 displays the evolution of R_H for the polyplex formulation of $N/P = 10$ as a function of time.

Figure 4 shows that the sizes the pDADMAC polyplexes with the lowest valences remain practically constant at around 85 nm during 7 days. By contrast, the DNA−p(1,1703), −p(1,2786), and −p(0.26,697) polyplexes, whose initial sizes were above 100 nm, seem to undergo a structural change with time. This structural rearrangement appears to be valence-dependent, since for the DNA−p(1,1703) system the size stabilization occurred from day 2 on, while for the DNA−p(1,2786) one it occurred from day 3 on. However, the final size was ca. 85 nm as in the case of the homologues. Such evolution has been ascribed in the literature to the presence of polymers with flexible chains. For the specific case of pDADMAC, Trzcinski et al. (ref 23 and references therein) report the stiffness *B*-parameter of pDADMAC as $0.17 \leq B \leq 0.28$, a rather high value compared to other polycations such as chitosan ($B < 0.1$). The authors conclude that the branching of high molecular weight commercial samples also contributes to an increase of this parameter, thereby resulting in a higher flexibility of the pDADMAC chain. In consequence, the observed size evolution of the DNA−pDADMAC polyplexes (accentuated with the increase in the cationic valence) may be related to both the branching of the pDADMAC polymer chain, expected to be present in a large extent,[21,22] and the low stiffness of pDADMAC,[23] which allows the polyplexes to undergo the structural rearrangement. For the coDADMAC polyplex, whose stabilization occurred from day 2 on and yielded a final size of roughly 120 nm, the same phenomenon is expected.

3.4. Isothermal Titration Calorimetry. The capability of DNA−polycation complexes to avoid premature dissociation from media and to promote the release of genetic material from the endosome once inside the cell is strongly related to the binding affinity between the DNA and the polycation in question.[31] The point (or points) on the DNA molecule to which the polycation binds is referred to as "binding site".

We investigated the DNA binding affinity of pDADMACs and coDADMAC via isothermal titration calorimetry (ITC) by

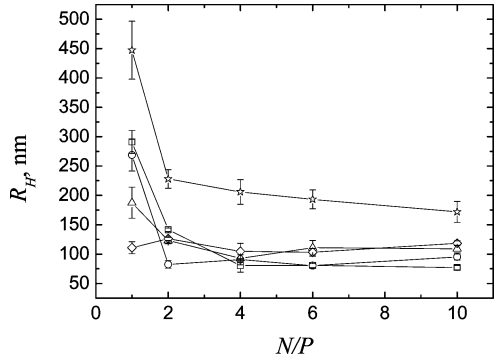

Figure 3. Hydrodynamic radius, R_H, of DNA polyplexes made with p(1,<619) (squares), p(1,919) (circles), p(1,1703) (triangles), p(1,2786) (diamonds), and p(0.26,697) (stars), as a function of the *N*/*P* molar ratio. Uncertainty bars represent the standard deviation of five runs.

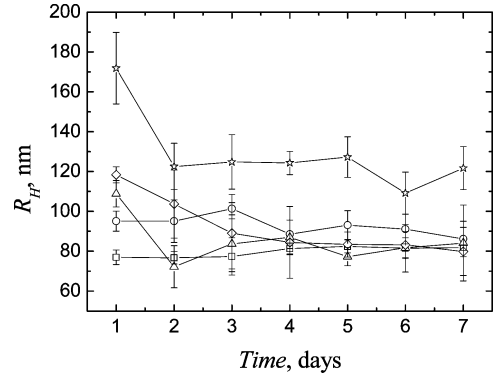

Figure 4. Hydrodynamic radius, R_H, of DNA polyplexes made with p(1,<619) (squares), p(1,919) (circles), p(1,1703) (triangles), p(1,2786) (diamonds), and p(0.26,697) (stars), as a function of time at a constant ratio $N/P = 10$. Uncertainty bars represent the standard deviation of five runs.

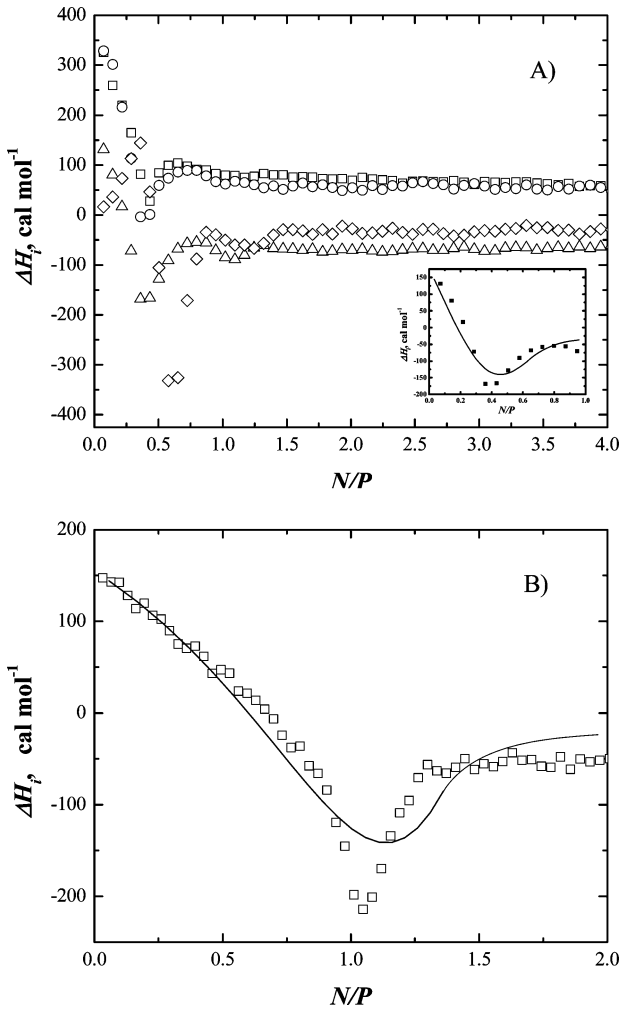

Figure 5. Integrated heats of interaction corrected for heats of dilution from the titration of p(1,<619) (squares), p(1,919) (circles), p(1,1703) (triangles), and p(1,2786) (diamonds) (A), and of p(0.26,697) (B), to DNA as a function of the *N*/*P* molar ratio. The solid lines in the inset of part A and in part B represent the two-site model fitting of the DNA−p(1,1703) and DNA−p(0.26,697) interactions, respectively.

titrating cationic ligand solutions to a DNA solution. It is well-known that ITC is an extremely sensitive technique in which the summation of several heat effects determines the shape of the binding isotherm. Such effects might include the dilution of both the polycation and DNA solutions, condensation and/or aggregation of the resultant polyplexes, coupled protonation effects, and possible conformational changes upon binding.[31,48] Consequently, aiming to obtain accurate thermodynamic binding parameters, the nonbinding heat contributions from the polymer dilution were subtracted before the curve-fitting algorithms were applied. On the other hand, it has to be noted that the heat originating from polycation protonation, observed in other systems,[49] is expected to be negligible in the present case considering that the pDADMAC cationic charge is pH-independent.[18−20]

Figure 5 shows the enthalpy of injection as a function of the *N*/*P* molar ratios for all of the polymers upon binding with DNA after the subtraction of polymer dilution effects. The solid lines in the inset of Figure 5A and in Figure 5B represent the two site model-fitting of the DNA−p(1,1703) and DNA−p(0.26,697) interactions, respectively. The fitting curves of the other DNA−pDADMAC complexes are not shown due to the similar shape they have with respect to the ones presented.

Three consecutive processes along the DNA−pDADMAC binding are observed in Figure 5A.

The first phase of binding occurred at *N*/*P* molar ratios lower than ∼1. An apparent biphasic nature of the binding profiles for all polymers (except for p(1,<619)) was observed. As the polymer chains began to saturate the DNA, the slightly endothermic binding enthalpy decreased and reached an exothermic minimum at an *N*/*P* molar ratio of ∼0.5. Nevertheless, for both minima and maxima, a slight shift to larger molar ratios was observed for the pDADMACs of higher valences. Similar slight endothermic heats observed for other DNA−cationic vector systems were ascribed to an entropy-driven binding process via counterion release upon binding.[12,50,51] Also, the positive enthalpy has also been described as a signature of ligand interaction to the DNA minor groove.[52] Concerning the reduction in ΔH_i observed, it results from the combination of both a decreased accessibility of binding sites to polymer molecules due to partial saturation of DNA molecules and from the dipole−dipole interactions between water molecules oriented favorably on adjacent DNA and polymer molecules.[53] At this stage, bending of single DNA strand, bridging of neighboring DNA molecules by polymer chains, and hydration can contribute to DNA collapse.[54]

The second phase of binding was characterized by an additional post-transition endothermic heat which finished in a maximum for pDADMACs at an *N*/*P* molar ratio of ∼0.75, with a subsequent decrease in enthalpy due to phosphate saturation. This endothermic heat increment with a subsequent peak or discontinuity has been suggested to represent DNA collapse,[12,55−57] and/or polyplex aggregation.[31,58] The increase in ΔH_i, from the zone in which DNA chains are partially saturated (the exothermic minimum) up to the observed maximum before phosphate saturation, is attributed to a binding of further polymer molecules to the partially saturated DNA. For the cases of p(1,1703) and p(1,2786), a subsequent secondary minimum and further little enthalpy increase can be found prior heat stabilization related to the complete phosphate saturation. These features that confirm what was observed by DLS (section 3.3) might indicate additional tertiary structural rearrangements of DNA molecules inside the complex and/or different polymer chain configuration in the complexes.

Finally, the third phase of binding was characterized by exothermic post-transition heats after complete phosphate saturation. The negative ΔH values observed for p(1,1703) and p(1,2786) might arise from the existence of local short-range electrostatic interactions between polymer molecules, polyplexes, and/or buffer ions. In contrast, the positive ΔH values observed for the DNA−p(1,<619) and DNA−p(1,929) binding experiments after subtraction of the heat of dilution led us to hypothesize that, even after phosphate saturation, there is some hydrophobic interaction between these two polymer molecules injected in excess and the polyplexes already formed.[57]

For the case of the DNA−coDADMAC complex formation (Figure 5B), only the first and third zones were observed as compared to the pDADMAC binding experiments. In good agreement with the conductometry (section 3.1) and DLS results (section 3.3), the exothermic minimum revealed that DNA condensation begins at a higher *N*/*P* molar ratio (∼1) compared to pDADMACs. This result confirms that (*N*/*P*)c is mainly governed by the cationic charge density.

In general, it is theorized that a higher binding affinity of ligand to the precollapsed form of DNA is a prerequisite for ligand-induced DNA collapse and condensation.[59] Moreover, it has also been assumed that the binding density increases with

TABLE 4: Thermodynamic Parameters of the Binding Interaction between DNA and pDADMAC[a]

polymer	$K_1 \times 10^{-5}$ (M^{-1})	n_1	ΔH_1 (kcal/mol)	ΔS_1 (kcal/(mol·K))
p(1,<619)	1.02 ± 0.26	0.44 ± 0.12	0.26 ± 0.07	0.023 ± 0.010
p(1,929)	3.10 ± 0.48	0.39 ± 0.11	0.20 ± 0.07	0.026 ± 0.010
p(1,1703)	51.6 ± 0.31	0.28 ± 0.07	0.07 ± 0.01	0.030 ± 0.005
p(1,2786)	55.1 ± 0.26	0.28 ± 0.07	0.06 ± 0.01	0.031 ± 0.005
p(0.26,668)	1.72 ± 0.14	0.86 ± 0.13	0.17 ± 0.03	0.024 ± 0.004
polymer	$K_2 \times 10^{-5}$ (M^{-1})	n_2	ΔH_2 (kcal/mol)	ΔS_2 (kcal/(mol·K))
p(1,<619)	0.06 ± 0.04	0.33 ± 0.10	2.34 ± 1.86	0.020 ± 0.013
p(1,929)	0.12 ± 0.07	0.26 ± 0.10	0.92 ± 0.74	0.022 ± 0.012
p(1,1703)	0.42 ± 0.08	0.15 ± 0.06	−0.40 ± 0.11	0.019 ± 0.05
p(1,2786)	0.43 ± 0.07	0.16 ± 0.06	−0.39 ± 0.11	0.020 ± 0.05
p(0.26,668)	0.17 ± 0.04	0.24 ± 0.04	−0.81 ± 0.07	0.020 ± 0.03

[a] Subscripts next to each parameter stand for the corresponding sites 1 and 2.

polymer concentration, and that DNA condenses and precipitates when the number of its neutralized charges reaches a critical value.[54,60,61] In this context, to distinguish between DNA condensation and DNA aggregation is a likely impossible task for mainly two reasons. First, aggregation per se is commonly accompanied by endothermic changes, and second, both phenomena can occur simultaneously.[31,62−64] Nevertheless, considering our coupled light scattering and ζ-potential data, we can derive that polyplex aggregation is not observed in this case since a decrease in hydrodynamic radii was observed while DNA condensation took place, and after that, the polyplex sizes remained constant at *N*/*P* ratios larger than 2, as also occurred for ζ-potential values. In addition, no precipitation was observed in the sample tubes after the samples were stored for more than 1 month (data not shown). Thus, on the basis of ITC, DLS and ζ-potential data, we can ascribe such endothermic increase to polymer-induced DNA condensation.

3.4.1. Thermodynamic Parameter Determination. The interpretation of calorimetric data involves the use of a model. The model, usually expressed as an equation or a set of equations, can be implemented for an arbitrary number of binding sites.[65,66] In general, there are three kinds of curve-fitting models, i.e., the single set of identical sites (SSIS) model, the two sets of independent sites (TSIS) model, and the sequential binding sites (SBS) model.[67] The SSIS describes properly many macromolecule−ligand binding systems when all the binding sites on the macromolecule are identical. The stoichiometry, *n*, binding constant, *K*, and change in enthalpy, ΔH, can be obtained. The TSIS model is implemented when the macromolecule has two kinds of binding sites. It enables the calculation of both sets of parameters n_1, K_1, ΔH_1, and n_2, K_2, ΔH_2 for the first and second sets of binding, respectively. Finally, the SBS model is appropriate for macromolecules possessing more than one kind of binding sites in which the binding of a ligand to one site will be influenced by whether or not ligands are bound to any of the other sites. *K* and ΔH are calculated from this model on each site.

In the present work, the DNA−pDADMAC binding process was assessed by employing the TSIS model supplied in the calorimeter (MicroCal Origin v. 5.0). The regions under study were those of $0 \leq N/P \leq 1$ and $0 \leq N/P \leq 1.5$ for pDADMACs and coDADMAC, respectively. The enthalpy, entropy, binding constant, and the stoichiometry of the interaction were derived. Results are summarized in Table 4.

We chose the TSIS model because the binding process of cationic ligands to DNA can be divided (as described previously in this section) into two main stages: a simple binding without a DNA conformational transition at first; and a binding event that takes place during the DNA conformational transition next.[68]

Analyzing the binding constants first, it can be observed from Table 4 that the values of K_1 and K_2 increased with pDADMAC valence. This increasing trend in both sets of constants demonstrates that the binding affinity is favored with pDADMAC valence. In good agreement with previously reported values for other cationic polymers[31,69] and many proteins,[70,71] the DNA binding constants obtained for all the polymers are on the order of 10^5-10^6 and 10^3-10^4 M^{-1} for the first and second sets of binding sites, respectively.

Regarding enthalpy, it is well-known that changes in it result from a combination of electrostatics, conformational changes (especially for second binding sites), and hydrogen-bonding interactions; therefore, ΔH cannot be strictly related to any one contribution. However, the DNA binding with all polymers showed slight enthalpic contributions (either positive or negative in sign) in both sites, revealing in consequence an entropically driven reaction typically observed in electrostatic polyelectrolyte associations promoted by the release of counterions upon attraction.[12,31,50,51] On the other hand, we speculate that the less favorable (more endothermic) ΔH_1 values associated with DNA−pDADMAC interaction may be a result of breaking hydrogen bonds between polymer and water molecules (breaking a hydrogen bond in water corresponds to an enthalpy increase of 1.9 kcal/mol).[72]

Finally, concerning entropy, the similar positive values observed in all binding experiments revealed that the charge interaction was analogous with a similar release of counterions upon binding. This result is consistent with the fact that all these polymers have the same number of amine groups within each repeat unit (one amine per repeat unit).

3.5. Atomic Force Microscopy. In order to illustrate the morphology of the polyplexes, tapping mode AFM in air was conducted. A volume of 50 μL of polyplexes at $N/P = 10$ was gently pipeted onto freshly cleaved mica, incubated during 2 min at room temperature, and dried by capillarity (without rinsing).

Figure 6A shows the results obtained for the DNA−p(0.26,697) polyplexes. A high population of well-defined toroids with diameters ranging from 125 to 250 nm is observed. These slightly smaller sizes compared to those obtained with DLS, given that we are looking at dry samples, suggest that polyplexes suffered dehydration once attached to the mica surface. For the polyplexes formed from pDADMACs, although to a lesser extent, also smaller sizes compared to DLS were revealed. Figure 6B shows a micrograph of the DNA−p(1,2786) polyplexes with diameters ranging from 80 to 200 nm.

DNA condensed in vitro can adopt a number of different morphologies of which the rodlike, globular, and toroidal ones are the most commonly observed. The reason for these differ-

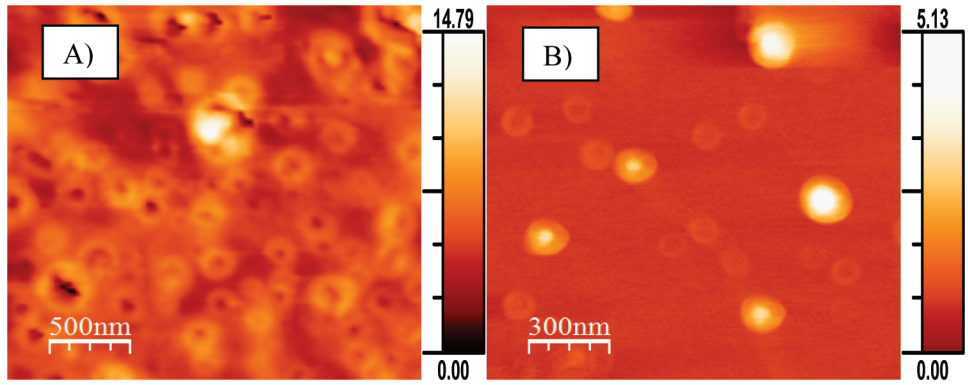

Figure 6. Height AFM images of DNA polyplexes made with p(0.26,697) (A), and with p(1,2786) (B) at a constant ratio $N/P = 10$. Bars next to images represent the Z scale in nm.

ences in morphology remains unclear; however, in good agreement with our results, the toroidal conformation seems to be exclusively linked to the polymer-mediated DNA compaction.[13]

3.6. Transfection Efficiency. Transfection efficiency was evaluated by the expression of the β-galactosidase and luciferase reporter enzymes. In order to avoid any kind of contamination related to the commercial polymer samples, two protocols prior to the polyplex formation were followed. On the one hand, polymers were sterile filtered (filter pore size of 0.22 μm, calcium acetate filter), and on the other hand, polymer solutions were added with 0.2 wt % of sodium azide (a biocide) and were left to incubate for at least 12 h. The polyplex formation and the subsequent transfection were conducted as described in section II. The (i) β-galactosidase (ONPG) and (ii) luciferase expression assays are described below.

(i) ONPG Assay for β-Galactosidase Expression. The potential of pDADMACs p(1,<619), p(1,2786), and p(0.26,668) as DNA carriers toward HeLa cells was evaluated. The polyplexes were formed at ratios in the range $0.5 \leq N/P \leq 18$. The ratios higher than 10 were evaluated based on the assumption that for efficient transfections a high excess of polycation is recommended.[73] In addition, MEP−DNA lipoplex (4:1 μL:μg) and naked DNA were measured as positive and negative controls, respectively. The specific activity, reported as the transfection efficiency, was calculated by dividing the sample absorbance by the product of the total protein mass obtained from the BCA assay (in milligrams) and the ONPG incubation time (in seconds).

Figure 7 shows the transfection efficiency of the polyplexes and controls as well as the protein content of the wells after lysation. It is clear that polyplexes within the whole range of ratios rendered levels of β-galactosidase expression comparable to that of the negative control (DNA without polymer). In general, their transfection efficiency seems to be favored at the higher ratios ($N/P \geq 6$); however, this apparent increase with polycation concentration cannot, in our opinion, be considered as conclusive because of the per se low responses.

On the other hand, it is well-known that the number of cells in culture is proportional to their protein release after lysation. In order to elucidate whether the low transfection efficiency was due to cytotoxic effects, the protein concentration was determined via the BCA assay. From Figure 7 a comparable level of protein content for all the formulations including the blanks was observed. Although not totally conclusive, this result shows that the cells proliferated approximately in the same way; consequently, the poor transfection efficiency shown by DNA−pDADMAC polyplexes compared to DNA−MEP lipoplexes cannot be related to cytotoxicity.

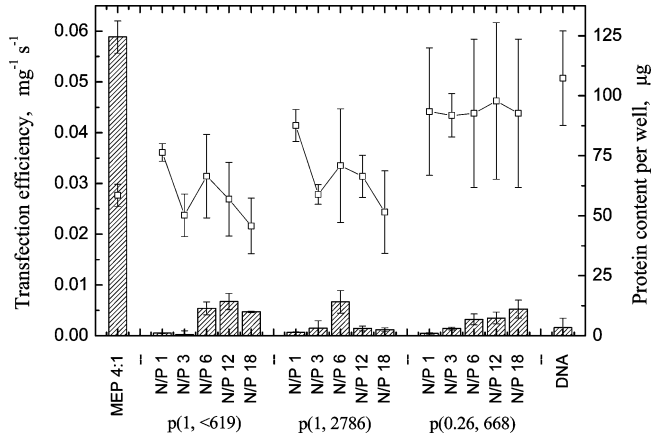

Figure 7. Transfection efficiency (columns) of DNA polyplexes made with p(1,<619), p(1,2786), and p(0.26,668) and protein content (squares) of wells after lysation. Uncertainty bars represent the standard deviation of three experiments.

To check whether the low transfection efficiency observed for all the polyplexes was brought about by the filtering of the polymers before the complexation, another protocol was proposed. As mentioned previously, 0.2 wt % sodium azide was added to pDADMAC solutions prior complexation. Transfection efficiencies and protein contents were comparable to those obtained with filtered samples (data not shown); hence, it could be concluded that the results did not depend on the polymer treatment.

(ii) Luciferase Expression Assay. The luciferase expression assay was conducted in order to confirm the results obtained by the β-galactosidase expression assay. The transfection efficiency for all cases was similar to that observed in the ONPG method. In general, naked DNA and the polyplexes regardless of the ratio yielded a luminescence of around 10 RLU, whereas DNA−MEP lipoplex yielded a luminescence of ca. 70×10^3 RLU Concerning the protein content determined by the BCA assay, the polyplexes rendered protein contents slightly higher than that of the DNA−MEP lipoplex (data not shown).

In consequence, the transfection efficiency of all pDADMAC polyplexes was confirmed to be low compared to the MEP lipoplex. Similar low transfer rates have been reported in the literature for other polymers with quaternized amines. Like DADMACs, quarternized poly(methacrylate)-based polymers showed efficient complex formation but poor transfection efficiency.[74,75] In previous studies, the poor transfection efficiency of pDADMACs has been related to a number of factors. While Fischer et al.[16] support that excess of polycation, even in the presence of chloroquine, limits the protein expression

due to in vitro cytotoxicity, other authors argue that the low tolerance to dissociation observed in DNA−pDADMAC polyplexes is presumably due to the bulky form of the quaternized groups.[76] However, the experimental results here presented suggest a different explanation. Based on the colloidal stability assessed by DLS and the positive ζ-potential observed, it is likely that the polyplexes, at least within the range of concentrations studied, exist in a form that is consistent with the "core−shell" structure of polymer-excessive complexes.[77] The model proposes that DNA is condensed in the inner part of the polyplex by the binding of short segments of a large number of polycation chains, whereas the remaining segments of these same chains are expected to be free in the outer part of the polyplexes. Consequently, as also exposed for other DNA−polycation systems,[78,79] the transfection efficiency of the DNA−pDADMAC polyplexes might be hampered by (i) the polycation barrier occurring in the core−shell structure proposed, (ii) the high binding affinity depicted by ITC (high binding constants), and (iii) the high stability exhibited by the polyplexes (DLS results). In this respect, Schaffer et al.[80] provide evidence that plasmid unpacking is indeed a limiting step for gene expression for sufficiently large polycation constructs. Also, Huth et al.[81] demonstrate that transfection efficiency of DNA−PEI polyplexes is higher for complexes with "intermediate" stability, which also gives support to our hypothesis.

IV. Conclusions

In this work, we studied poly(diallyldimethylammonium chloride) (pDADMAC) as a DNA carrier. Particular attention was paid to the influence of its charge density, CD, and valence on the DNA compaction and subsequent transfection. While the cationic charge density was demonstrated to govern the DNA compaction ratio, (N/P)c, the valence proved to influence both the overall size of the polyplexes and the ratio from which these sizes remain practically constant, $(N/P)^*$. In addition, a size restructuring of the polyplexes with time was ascribed to the flexibility of the cationic polymer chain, which in turn can be attributed to the valence (molecular weight).

From a physicochemical point of view, the DNA−pDADMAC polyplexes revealed promising results toward transfection for $N/P \geq 2$; however, the transfection efficiency, regardless of N/P, CD, and valence, was low compared to the DNA−Metafectene Pro lipoplex tested as a blank.

At present, the low transfection efficiency of the polyplexes, considering the good colloidal properties they have, seems to be explained by (i) the polycation barrier occurring in the core−shell structure proposed, (ii) the high binding affinity depicted by ITC (high binding constants), and (iii) the high stability exhibited by the polyplexes (DLS results). Nevertheless, a deeper understanding of the DNA decompaction process inside the cell must, in our opinion, be achieved.

Acknowledgment. The authors are grateful to the Department of Physical Chemistry 1, Center for Chemistry and Chemical Engineering, Lund University, to Dr. Ulf Olsson in particular for lending AFM facilities and for his fruitful discussions.

The authors also thank Dr. Alfredo González-Perez (University of Southern Denmark) and Luis Pegado (Lund University) for their valuable assistance.

J.R.R. thanks the Dirección Xeral de I+D+I of the Xunta de Galicia and the European Regional Development Fund (INCITE07PXI206076ES) for the financial supports. P.T. thanks the Xunta de Galicia for financial support by project INCITE 09206020PR.

M.A.-M. is supported by the Programme Alban, the European Union Programme of High Level Scholarships for Latin America, scholarship No. (E06D101860MX).

References and Notes

(1) Gonzalez-Perez, A.; Dias, R. S. *Front Biosci. (Elite Ed)* **2009**, *1*, 228.
(2) Crystal, R. G. *Nat. Med.* **1995**, *1*, 15.
(3) Verma, I. M.; Somia, N. *Nature* **1997**, *389*, 239.
(4) Luo, D.; Saltzman, W. M. *Nat. Biotechnol.* **2000**, *18*, 33.
(5) Fraley, A. W.; Pons, B.; Dalkara, D.; Nullans, G.; Behr, J. P.; Zuber, G. *J. Am. Chem. Soc.* **2006**, *128*, 10763.
(6) Niidome, T.; Huang, L. *Gene Ther.* **2002**, *9*, 1647.
(7) Midoux, P.; Pichon, C.; Yaouanc, J. J.; Jaffres, P. A. *Br. J. Pharmacol.* **2009**, *157*, 166.
(8) Dias, R. S., Lindman, B., Eds.; *DNA Interactions with Polymers and Surfactants*; Wiley-Interscience: New York, 2008.
(9) Liverpool, T. B.; Stapper, M. *Europhys. Lett.* **1997**, *40*, 485.
(10) Dobrynin, A. V.; Colby, R. H.; Rubinstein, M. *Macromolecules* **1995**, *28*, 1859.
(11) Manning, G. S. *Q. Rev. Biophys.* **1978**, *11*, 179.
(12) Matulis, D.; Rouzina, I.; Bloomfield, V. A. *J. Mol. Biol.* **2000**, *296*, 1053.
(13) De Smedt, S. C.; Demeester, J.; Hennink, W. E. *Pharm. Res.* **2000**, *17*, 113.
(14) Borchard, G. *Adv. Drug Delivery Rev.* **2001**, *52*, 145.
(15) Jiang, H.; Taranekar, P.; Reynolds, J. R.; Schanze, K. S. *Angew. Chem., Int. Ed.* **2009**, *48*, 4300.
(16) Fischer, D.; Dautzenberg, H.; Kunath, K.; Kissel, T. *Int. J. Pharm.* **2004**, *280*, 253.
(17) Krajcik, R.; Jung, A.; Hirsch, A.; Neuhuber, W.; Zolk, O. *Biochem. Biophys. Res. Commun.* **2008**, *369*, 595.
(18) Jaeger, W.; Hahn, M.; Lieske, A.; Zimmermann, A.; Brand, F. *Macromol. Symp.* **1996**, *111*, 95.
(19) Dautzenberg, H.; Gornitz, E.; Jaeger, W. *Macromol. Chem. Phys.* **1998**, *199*, 1561.
(20) Dautzenberg, H. *Macromol. Chem. Phys.* **2000**, *201*, 1765.
(21) Xia, J. L.; Dubin, P. L.; Edwards, S.; Havel, H. *J. Polym. Sci., Part B: Polym. Phys.* **1995**, *33*, 1117.
(22) Wandrey, C.; Hernandez-Barajas, J.; Hunkeler, D. *Radical Polym. Polyeletrolytes* **1999**, *145*, 123.
(23) Trzcinski, S.; Varum, K. M.; Staszewska, D. U.; Smidsrod, O.; Bohdanecky, M. *Carbohydr. Polym.* **2002**, *48*, 171.
(24) Marcelo, G.; Tarazona, M. P.; Saiz, E. *Polymer* **2005**, *46*, 2584.
(25) Saenger, W. *Principles of Nucleic Acid Structure*; Springer-Verlag: New York, 1984.
(26) Felgner, P. L.; Barenholz, Y.; Behr, J. P.; Cheng, S. H.; Cullis, P.; Huang, L.; Jessee, J. A.; Seymour, L.; Szoka, F.; Thierry, A. R.; Wagner, E.; Wu, G. *Hum. Gene Ther.* **1997**, *8*, 511.
(27) Camp, J. P.; Capitano, A. T. *Biophys. Chem.* **2005**, *113*, 115.
(28) Provencher, S. W. *Comput. Phys. Commun.* **1982**, *27*, 213.
(29) Alatorre-Meda, M.; Taboada, P.; Sabin, J.; Krajewska, B.; Varela, L. M.; Rodriguez, J. R. *Colloids Surf. A−Physicochem. Eng. Aspects* **2009**, *339*, 145.
(30) Pecora, R. *Dynamic Light Scattering*; Plenum Press: New York, 1985.
(31) Prevette, L. E.; Kodger, T. E.; Reineke, T. M.; Lynch, M. L. *Langmuir* **2007**, *23*, 9773.
(32) Horcas, I.; Fernandez, R.; Gomez-Rodriguez, J. M.; Colchero, J.; Gomez-Herrero, J.; Baro, A. M. *Rev. Sci. Instrum.* **2007**, 78.
(33) Dias, R. S.; Magno, L. M.; Valente, A. J. M.; Das, D.; Das, P. K.; Maiti, S.; Miguel, M. G.; Lindman, B. *J. Phys. Chem. B* **2008**, *112*, 14446.
(34) Rodriguez-Pulido, A.; Aicart, E.; Llorca, O.; Junquera, E. *J. Phys. Chem. B* **2008**, *112*, 2187.
(35) Felgner, P. L.; Tsai, Y. J.; Sukhu, L.; Wheeler, C. J.; Manthorpe, M.; Marshall, J.; Cheng, S. H. *DNA Vaccines* **1995**, *772*, 126.
(36) Dias, R. S.; Lindman, B.; Miguel, M. G. *J. Phys. Chem. B* **2002**, *106*, 12600.
(37) Lasic, D. D.; Templeton, N. S. *Adv. Drug Delivery Rev.* **1996**, *20*, 221.
(38) Radler, J. O.; Koltover, I.; Salditt, T.; Safinya, C. R. *Science* **1997**, *275*, 810.
(39) Tang, M. X.; Szoka, F. C. *Gene Ther.* **1997**, *4*, 823.
(40) Pouton, C. W.; Lucas, P.; Thomas, B. J.; Uduehi, A. N.; Milroy, D. A.; Moss, S. H. *J. Controlled Release* **1998**, *53*, 289.
(41) Toncheva, V.; Wolfert, M. A.; Dash, P. R.; Oupicky, D.; Ulbrich, K.; Seymour, L. W.; Schacht, E. H. *Biochim. Biophys. Acta−Gen. Subj.* **1998**, *1380*, 354.
(42) Maruyama, A.; Katoh, M.; Ishihara, T.; Akaike, T. *Bioconjugate Chem.* **1997**, *8*, 3.

(43) Wolfert, M. A.; Schacht, E. H.; Toncheva, V.; Ulbrich, K.; Nazarova, O.; Seymour, L. W. *Hum. Gene Ther.* **1996**, *7*, 2123.
(44) Dias, R. S.; Innerlohinger, J.; Glatter, O.; Miguel, M. G.; Lindman, B. *J. Phys. Chem. B* **2005**, *109*, 10458.
(45) MacLaughlin, F. C.; Mumper, R. J.; Wang, J. J.; Tagliaferri, J. M.; Gill, I.; Hinchcliffe, M.; Rolland, A. P. *J. Controlled Release* **1998**, *56*, 259.
(46) Nuno-Donlucas, S. M.; Sanches-Diaz, J. C.; Rabelero, M.; Cortes-Ortega, J.; Luhrs-Olmos, C. C.; Fernandez-Escamilla, V. V.; Mendizabal, E.; Puig, J. E. *J. Colloid Interface Sci.* **2004**, *270*, 94.
(47) Puig, L. J.; Sanchez-Diaz, J. C.; Villacampa, M.; Mendizabal, E.; Puig, J. E.; Aguiar, A.; Katime, I. *J. Colloid Interface Sci.* **2001**, *235*, 278.
(48) Wiseman, T.; Williston, S.; Brandts, J. F.; Lin, L. N. *Anal. Biochem.* **1989**, *179*, 131.
(49) Ma, P. L.; Lavertu, M.; Winnik, F. M.; Buschmann, M. D. *Biomacromolecules* **2009**, *10*, 1490.
(50) Srinivasachari, S.; Liu, Y. M.; Prevette, L. E.; Reineke, T. M. *Biomaterials* **2007**, *28*, 2885.
(51) Prevette, L. E.; Lynch, M. L.; Reineke, T. M. *Biomacromolecules* **2010**, *11*, 326.
(52) Privalov, P. L.; Dragan, A. I.; Crane-Robinson, C.; Breslauer, K. J.; Remeta, D. P.; Minetti, C. *J. Mol. Biol.* **2007**, *365*, 1.
(53) Strey, H. H.; Podgornik, R.; Rau, D. C.; Parsegian, V. A. *Curr. Opin. Struct. Biol.* **1998**, *8*, 309.
(54) Rau, D. C.; Parsegian, V. A. *Biophys. J.* **1992**, *61*, 246.
(55) Huang, D.; Korolev, N.; Eom, K. D.; Tam, J. P.; Nordenskiold, L. *Biomacromolecules* **2008**, *9*, 321.
(56) Coles, D. J.; Yang, S.; Minchin, R. F.; Toth, I. *Biopolymers* **2008**, *90*, 651.
(57) Patel, M. M.; Anchordoquy, T. J. *Biophys. J.* **2005**, *88*, 2089.
(58) Prevette, L. E.; Lynch, M. L.; Kizjakina, K.; Reineke, T. M. *Langmuir* **2008**, *24*, 8090.
(59) Lando, D. Y.; Teif, V. B. *J. Biomol. Struct. Dyn.* **2002**, *20*, 215.
(60) Porschke, D. *Biochemistry* **1984**, *23*, 4821.
(61) Ehtezazi, T.; Rungsardthong, U.; Stolnik, S. *Langmuir* **2003**, *19*, 9387.
(62) Srinivasachari, S.; Liu, Y. M.; Zhang, G. D.; Prevette, L.; Reineke, T. M. *J. Am. Chem. Soc.* **2006**, *128*, 8176.
(63) Taboada, P.; Mosquera, V.; Attwood, D.; Yang, Z.; Booth, C. *Phys. Chem. Chem. Phys.* **2003**, *5*, 2625.
(64) Alvarez-Lorenzo, C.; Barreiro-Iglesias, R.; Concheiro, A.; Iourtchenko, L.; Alakhov, V.; Bromberg, L.; Temchenko, M.; Deshmukh, S.; Hatton, T. A. *Langmuir* **2005**, *21*, 5142.
(65) Roselin, L. S.; Lin, M. S.; Lin, P. H.; Chang, Y.; Chen, W. Y. *Biotechnol. J.* **2010**, *5*, 85.
(66) Freire, E.; Schon, A.; Velazquez-Campoy, A. *Methods Enzymol.: Biothermodyn.* **2009**, *455* (Part A), 127.
(67) Freire, E.; Mayorga, O. L.; Straume, M. *Anal. Chem.* **1990**, *62*, A950.
(68) Kim, W.; Yamasaki, Y.; Kataoka, K. *J. Phys. Chem. B* **2006**, *110*, 10919.
(69) Nisha, C. K.; Manorama, S. V.; Ganguli, M.; Maiti, S.; Kizhakkedathu, J. N. *Langmuir* **2004**, *20*, 2386.
(70) Milev, S.; Bosshard, H. R.; Jelesarov, I. *Biochemistry* **2005**, *44*, 285.
(71) Engler, L. E.; Welch, K. K.; JenJacobson, L. *J. Mol. Biol.* **1997**, *269*, 82.
(72) Silverstein, K. A. T.; Haymet, A. D. J.; Dill, K. A. *J. Am. Chem. Soc.* **2000**, *122*, 8037.
(73) Fischer, D.; Bieber, T.; Li, Y. X.; Elsasser, H. P.; Kissel, T. *Pharm. Res.* **1999**, *16*, 1273.
(74) Wolfert, M. A.; Dash, P. R.; Nazarova, O.; Oupicky, D.; Seymour, L. W.; Smart, S.; Strohalm, J.; Ulbrich, K. *Bioconjugate Chem.* **1999**, *10*, 993.
(75) Arigita, C.; Zuidam, N. J.; Crommelin, D. J. A.; Hennink, W. E. *Pharm. Res.* **1999**, *16*, 1534.
(76) Izumrudov, V. A.; Zhiryakova, M. V.; Kudaibergenov, S. E. *Biopolymers* **1999**, *52*, 94.
(77) Kabanov, A. V.; Kabanov, V. A. *Adv. Drug Delivery Rev.* **1998**, *30*, 49.
(78) Schaffert, D.; Wagner, E. *Gene Ther.* **2008**, *15*, 1131.
(79) Chen, H. H.; Ho, Y. P.; Jiang, X.; Mao, H. Q.; Wang, T. H.; Leong, K. W. *Molecular Therapy* **2008**, *16*, 324.
(80) Schaffer, D. V.; Fidelman, N. A.; Dan, N.; Lauffenburger, D. A. *Biotechnol. Bioeng.* **2000**, *67*, 598.
(81) Huth, S.; Hoffmann, F.; von Gersdorff, K.; Laner, A.; Reinhardt, D.; Rosenecker, J.; Rudolph, C. *J. Gene Med.* **2006**, *8*, 1416.

JP1016856